International Journal of Computer Vision, 8:1, 53–69 (1992)

Qualitative Surface Shape from Deformation of Image Curves

ROBERTO CIPOLLA* AND ANDREW ZISSERMAN
Department of Engineering Science, University of Oxford, Oxford OX1 3PJ

Received April 12, 1991. Revised March 10, 1992.

Abstract
We describe the constraints placed on the differential geometry of a surface by observing a surface curve from a sequence of positions. In particular two new qualitative results are presented. First, it is shown that sign of normal curvature along the surface curve is determined by tracking image curve inflections. This result requires only approximate knowledge of the direction of projected viewer translation. It is a generalization to surface curves of Weinshall's [28] result for surface texture. Second, it is shown that surface orientation at a transverse crossing of surface curves is determined without knowledge of viewer translation. Results are demonstrated on real image sequences.

1 Introduction

Imagine we have several views of a curve lying on a surface. If the motion between the views and the camera calbiration are known then in principle it is possible to reconstruct this space curve from its projections. It is also possible in principle to determine the curve's tangent and curvature. In practice this requires precise calibration of epipolar geometry and subpixel accuracy for edge localization and/or integrating information over many views in order to reduce discretization errors. However, even if perfect reconstruction could be achieved, the end result would only be a space curve. This delimits the surface only in the way that a rigid net restricts a rubber plate [15]—the rubber can bulge through the net, with varying surface orientation. If instead of a net of space curves we have a net of *surface strips* [20], where both position and normal are known, the bulge of the plate is severely restricted. Conversely, such information enables grouping of curves into coherent surfaces.

Here we analyze the images of surface curves (contours generated from internal surface markings or illumination effects) and investigate the surface geometric information available from the temporal evolution of their image under viewer motion. In particular we determine constraints on surface geometry using only *qualitative* knowledge of viewer motion, that is, using only information that can be recovered efficiently and robustly, without requiring exact knowledge of viewer motion or accurate image measurements. The description is, however, incomplete.

Certain curves and tracked points are rich sources of surface geometry. At an apparent contour (the image of the points where the viewing direction lies in the tangent plane) the surface normal is known [1]. Further, the curvature of the apparent contour in a single view determines the sign of the Gaussian curvature of the surface projecting to the contour [6, 19]. From the deformation of the apparent contour under viewer motion a surface patch (first and second fundamental forms) can be recovered [3, 11, 14, 26]. A self-shadow (where the illuminant direction lies in the tangent plane) can be exploited in a similar manner if the illuminant position is known [20]. Tracking specular points [30] gives a surface strip along which the surface normal is known.

Surface curves have three advantages over isolated surface markings:

1. **Sampling:** Isolated texture only "samples" the surface at isolated points; between the points, the

*Toshiba Fellow, Toshiba Corporation, Research and Development Center, Kawasaki 210, Japan.

surface could have any shape. Conversely, a surface curve conveys information at a particular scale through its path.

2. **Geometric Structure:** Curves, unlike points, have well-defined tangents which constrain surface orientation.
3. **Technological:** There are now available reliable, accurate edge detectors which localize surface markings to subpixel accuracy [9]. The technology for isolated point detection is not at such an advanced stage. Furtheremore, snakes [18] are ideally suited to tracking curves through a sequence of images, and thus measuring curve deformation.

Here we are not concerned with *distinguishing* surface curves from other curves such as extremal boundaries (though this may be carried out by their differing deformation under viewer motion [11, 26], rather than on photometric grounds) or from surface creases or space curves (such as a piece of wire), where surface orientation is not defined. We analyze the spatiotemporal family of image contours generated under viewer motion to derive constraints on surface shape. We do not consider the complementary problem of determining constraints on the viewer motion from the visual motion of the surface curve [10, 13].

This article is divided into three parts. First, in section 2, the geometry of space curves is reviewed and related to the perspective image. In particular, a simple expression for the curvature of the image contour is derived. Second, in section 3, the information available from the deformation of the image curve under viewer motion is investigated, making explicit the constraints that this imposes on the geometry of the space curve. Third, in section 4, the aspects of the differential geometry of the surface that can be gleaned by knowing that the curve lies on the surface are discussed.

It is shown that *visibility* of points on the curve constrains, but does not determine surface normal. This constraint is tightened by including the restriction imposed by the tangent of the surface curve. Furthermore, certain 'events' (inflections, transverse curve crossings) are richer still in geometric information. In particular it is shown that (1) tracking image curve inflections determines the sign of normal curvature in the direction of the surface curve's tangent vector; and (2) surface orientation at transverse curve crossing requires only knowledge of viewer orientation, not position. The first result is a generalization to surface curves of Weinshall's [28, 29] result for surface texture. Examples are included for real-image sequences.

2 The Perspective Projection of Space Curves

2.1 Review of Space Curve Geometry

Consider a point P on a regular differentiable curve $\mathbf{r}(s)$ in R^3 (figure 1). The local geometry of the curve is uniquely determined in the neighborhood of P by the basis of unit vectors $\{\mathbf{T}, \mathbf{N}, \mathbf{B}\}$, the curvature, κ, and torsion, τ, of the space curve [12]. For an arbitrary parameterization of the curve, $\mathbf{r}(s)$, these quantities are defined in terms of the derivatives (up to third order) of the curve with respect to the parameter s. The first-order derivative ("velocity") is used to define the tangent to the space curve, $\mathbf{T}$, a unit vector given by

$$\mathbf{T} = \frac{\mathbf{r}_s}{|\mathbf{r}_s|} \tag{1}$$

The second-order derivative—in particular the component perpendicular to the tangent ("centripetal acceleration")—is used to define the curvature, κ (the magnitude) and the curve normal, $\mathbf{N}$ (the direction):

$$\kappa\mathbf{N} = \frac{(\mathbf{T} \wedge \mathbf{r}_{ss}) \wedge \mathbf{T}}{|\mathbf{r}_s|^2} \tag{2}$$

The plane spanned by $\mathbf{T}$ and $\mathbf{N}$ is called the *osculating plane*. This is the plane that $\mathbf{r}(s)$ is closest to lying in (and does lie in if the curve has no torsion). These two vectors define a natural frame for describing the geometry of the space curve. A third vector, the binormal $\mathbf{B}$, is chosen to form a right-handed set:

$$\mathbf{B} = \mathbf{T} \wedge \mathbf{N} \tag{3}$$

This leaves only the torsion of the curve, defined in terms of the deviation of the curve out of the osculating plane:

$$\tau = \frac{\mathbf{r}_{sss} \cdot \mathbf{B}}{\kappa\,|\mathbf{r}_s|^3} \tag{4}$$

The relationship between these quantitites and their derivatives for movements along the curve can be conveniently packaged by the Frenet-Serret equations [12] which for an arbitrary parameterization are given by

$$\mathbf{T}_s = |\mathbf{r}_s|\kappa\mathbf{N} \tag{5}$$

$$\mathbf{N}_s = |\mathbf{r}_s|(-\kappa\mathbf{T} + \tau\mathbf{B}) \tag{6}$$

$$\mathbf{B}_s = -|\mathbf{r}_s|\tau\mathbf{N} \tag{7}$$

The influence of curvature and torsion on the shape of a curve are clearly demonstrated in the Taylor series expansion about a point u_0 on the curve.

$$\mathbf{r}(u) = \mathbf{r}(u_0) + u\mathbf{r}_u(u_0) + \frac{u^2}{2}\mathbf{r}_{uu}(u_0) + \frac{u^3}{6}\mathbf{r}_{uuu}(u_0) + \ldots \quad (8)$$

where u is an arc length parameter of the curve. An approximation for the curve with the lowest order in u along each basis vector is given by [20]

$$\mathbf{r}(u) = \mathbf{r}(u_0) + (u + \ldots)\mathbf{T} + \left(\frac{u^2}{2} + \cdots\right)\kappa\mathbf{N} + \left(\frac{u^3}{6} + \cdots\right)\kappa\tau\mathbf{B} \quad (9)$$

The zero-oder term is simply the fiducial point itself; the first-order term is a straight line along the tangent direction; the second-order term is a parabolic arc in the osculating plane; and the third-order term describes the deviation from the osculating plane. Projection on to planes perpendicular to **T**, **N**, **B** give the local forms shown in figure 1. It is easy to see from (9) that the orthographic projection on to the **T** − **N** plane (osculating plane) is a parabolic arc; on the **T** − **B** plane an inflection; and the projection on the **N** − **B** plane is a *cusped* curve. If κ or τ are zero then higher order terms are important and the local forms must be modified. These local forms illustrate how the apparent shape of a space curve changes with different viewpoints. The exact relationship between the space curve geometry and its image under perspective projection will now be derived.

2.2 *Imaging Model*

A monocular observer can determine the orientation of any ray projected on to its imaging surface. The observer cannot however, determine the distance along the ray of the object feature that generated it. A general model for the imaging device is therefore to consider it as determining the direction of an incoming ray which we can choose to represent as a unit vector. The imaging device is then equivalent to a spherical pin-hole camera of unit radius. The advantage of this approach (over planar representation) is that formulas under perspective are often as simple as (or identical to) those under orthographic projection [3, 11, 22].

Consider perspective projection on to a sphere of unit radius as shown in figure 2. The image of a world point, P, with position vector, $\mathbf{r}(s)$, is a unit vector $\mathbf{Q}(s, t)$ such that

$$\mathbf{r}(s) = \mathbf{v}(t) + \lambda(s, t)\mathbf{Q}(s, t) \quad (10)$$

where s is a parameter along the image curve; t is chosen to index the view (corresponding to time or viewer position); $\lambda(s, t)$ is the distance along the ray to P; and $\mathbf{v}(t)$ is the viewer position (center of spherical

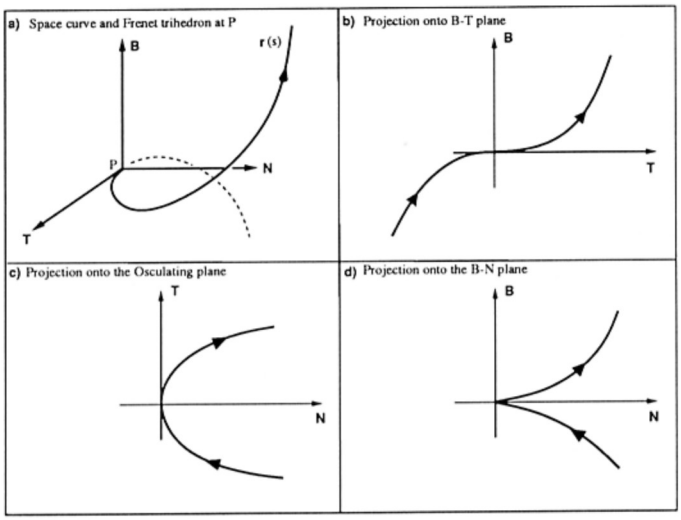

Fig. 1. Space curve geometry and local forms of its projection. The local geometry of a space curve can be completely specified by the Frenet trihedron of vectors {**T**, **N**, **B**}, the curvature, κ, and torsion, τ, of the curve. Projection of the space curve onto planes perpendicular to these vectors (the local canonical forms [12]) illustrates how the apparent shape of a space curve changes with different viewpoints.

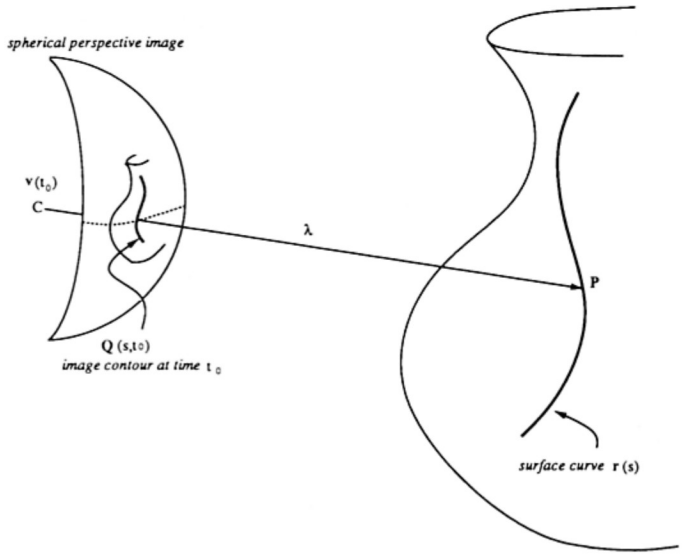

Fig. 2. Viewing and surface geometry. The image defines the direction of a ray, (unit vector **Q**) to a point, **P**, on a surface cruve, $\mathbf{r}(s)$. The distance from the viewer (center of projection sphere $\mathbf{v}(t)$) to **P** is λ.

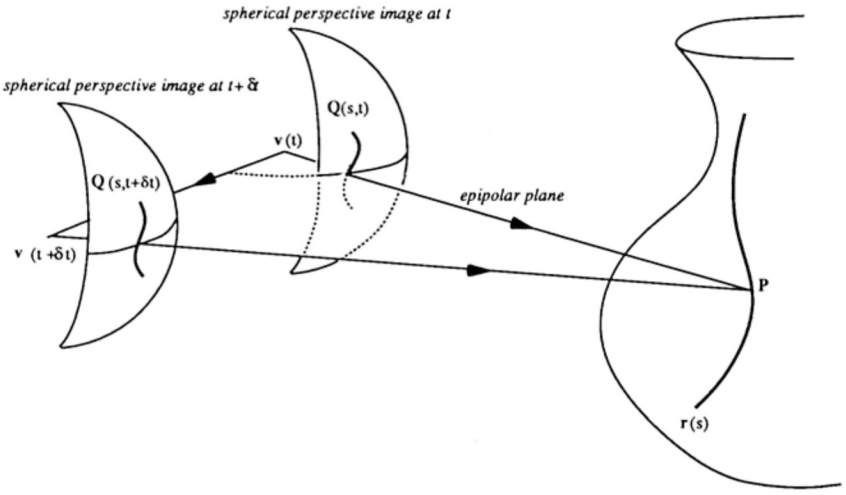

Fig. 3. Epipolar geometry. A moving observer at position $\mathbf{v}(t)$ sees a one-parameter family of image curves, $\mathbf{Q}(s, t)$—the spherical perspective projections of a space curve, $\mathbf{r}(s)$, indexed by time.

pin-hole camera) at time t. A moving monocular observer at position $\mathbf{v}(t)$ sees a family of views of the curve indexed by time, $\mathbf{Q}(s, t)$ (see figure 3).[1]

2.3 Relating Image and Space Curve Geometry

Equation (10) gives the relationship between a point on the curve, $\mathbf{r}(s)$, and its spherical perspective projection, $\mathbf{Q}(s, t)$, for a view indexed by time t. It can be used to relate the space curve geometry (**T**, **N**, **B**, κ, τ) to the image and viewing geometry. The relationship between the orientation of the curve and its image tangent and the curvature of the space curve and its projection are now described.

2.3.1 Image Curve Tangent and Normal. At the projection of P, the tangent to the spherical image curve, $\mathbf{t}^p$, is related to the space curve tangent **T** and the viewing geometry by

$$\mathbf{t}^p = \frac{\mathbf{T} - (\mathbf{Q} \cdot \mathbf{T})\mathbf{Q}}{[1 - (\mathbf{Q} \cdot \mathbf{T})^2]^{1/2}} \tag{11}$$

This relationship is derived in appendix A.

The direction of the ray, $\mathbf{Q}$, and the image curve tangent, $\mathbf{t}^p$, determine the orientation of the spherical image curve normal, $\mathbf{n}^p$:

$$\mathbf{n}^p = \mathbf{Q} \wedge \mathbf{t}^p \tag{12}$$

2.3.2 Curvature of Projection. The curvature of the image curve, κ^p defined as the *geodesic* curvature of the spherical curve, $\mathbf{Q}(s, t)$—

$$\kappa^p = \frac{\mathbf{Q}_{ss} \cdot \mathbf{n}^p}{|\mathbf{Q}_s|^2} \tag{13}$$

is related to the space curve curvature, κ, and the viewing geometry by

$$\kappa^p = \lambda\kappa \frac{[\mathbf{Q}, \mathbf{T}, \mathbf{N}]}{[1 - (\mathbf{Q} \cdot \mathbf{T})^2]^{3/2}} \tag{14}$$

where $[\mathbf{Q}, \mathbf{T}, \mathbf{N}]$ represents the triple scalar product.[2] (See appendix A for a derivation). Note that the numerator depends on the angle between the ray and the osculating plane. The denominator depends on the angle between the ray and the curve tangent.

A similar result is described in [20]. Under orthographic projection the expression is the same apart from the scaling factor of λ. As expected, the image curvature scales linearly with distance and is proportional to the space curve curvature κ. More importantly, the sign of the curvature of the projection depends on which side of the osculating plane the ray $\mathbf{Q}$ lies, that is, on the sign of the scalar product $\mathbf{B} \cdot \mathbf{Q}$. This is easily seen to be true by viewing a curve drawn on a sheet of paper from both sides. The case in which the vantage point is in the osculating plane corresponds to a zero of curvature in the projection. From equation (14) (see also [27]) the projected curvature will be zero if and only if

1. $\kappa = 0$
   The curvature of the space curve is zero. This does not occur for generic curves [7]. The local form depends on terms higher than second in the Taylor expansion (9).
2. $[\mathbf{Q}, \mathbf{T}, \mathbf{N}] = 0$ with $\mathbf{Q} \cdot \mathbf{T} \neq 0$
   The view direction lies in the osculating plane, but not along the tangent to the curve (if the curve is projected along the tangent the image is, in general, a cusp). Provided the torsion is not zero, $\mathbf{r}(s)$ crosses its osculating plane, seen in the image as a zero crossing.

Inflections will occur generically (i.e., stable to a small perturbation of the curve or viewing position) in any view of a curve, but cusps only become generic in a one-parameter family of views [7][3]. Inflections in image curves are therefore more likely to be consequences of the viewing geometry (condition 2 above) than zeros of the space curve curvature (condition 1). This severely limits the power of inflections of image curves as invariants of perspective projection of space curves [27].

3 Deformation Due to Viewer Movements

As the viewer moves, the image of $\mathbf{r}(s)$ will deform. The deformation is characterized by a change in image position (image velocities), a change in image curve orientation, and a change in the curvature of the projection. In appendix B we derive expressions relating the deformation of the image curve to the space curve geometry and then show how the space curve tangent and curvature can be calculated directly from image measurables when the viewer motion is known without having to explicitly reconstruct the space curve and differentiate. In particular the temporal derivative of the image curve's position (image velocity), orientation, and curvature can be used to recover the space curves position (depth, λ), tangent ($\mathbf{T}$) and curvature ($\kappa\mathbf{N}$).

Here we investigate the relationship between the temporal derivative of the image curvature, κ_t^p, and the space curve geometry (derivation in appendix B):

$$\kappa_t^p = -\frac{\kappa\mathbf{B} \cdot \mathbf{U}}{[1 - (\mathbf{Q} \cdot \mathbf{T})^2]^{3/2}} - \frac{3\kappa^p[(\mathbf{Q} \cdot \mathbf{T})(\mathbf{U} \cdot \mathbf{t}^p)]}{\lambda[1 - (\mathbf{Q} \cdot \mathbf{T})^2]^{1/2}} \tag{15}$$

where $\mathbf{U} = \mathbf{v}_t$ is the viewer's translational velocity. Note that the measurement of κ_t^p requires matching the image of a point on the space curve over the sequence of views/time.

In the special case of viewing a section of curve that projects to an inflection, that is, $\kappa^p = 0$, or for viewer motion in a direction perpendicular to the image curve's tangent, that is, $\mathbf{U} \cdot \mathbf{t}^p = 0$, the second term in (15) is zero and

$$\kappa_t^p = -\frac{\kappa\mathbf{B} \cdot \mathbf{U}}{[1 - (\mathbf{Q} \cdot \mathbf{T})^2]^{3/2}} \tag{16}$$

that is, the sign of the deformation of the image curve encodes the sign of $\mathbf{B} \cdot \mathbf{U}$ (since κ and the denominator are always positive). This is sufficient to determine what the curve normal is doing qualitatively, that is, whether

the curve is bending toward or away from the viewer. This information is used in secction 4.3 to recover qualitative properties of the underlying surface's shape.

If the image curve at time t has a zero of curvature because $\mathbf{Q}$ lies in the osculating plane, the inflection will not disappear in general under viewer motion but will move along the image curve, corresponding to *movement* of its preimage along the space curve (see later, figure 8). Generically inflections can only be created or annihilated in pairs [8].

4 Surface Geometry

4.1 Visibility Constraint

Since the curve is visible, the angle between the surface normal and the line of sight must be less than or equal to 90° (otherwise the local tangent plane would occlude the curve). If the angle is 90° then the image curve is coincident with the apparent contour of the surface.

The visibility constraint can be utilized to constrain surface orientation, $\mathbf{n}$. Since,

$$-1 \leq \mathbf{Q} \cdot \mathbf{n} \leq 0 \tag{17}$$

if $\mathbf{Q}$ is taken as the south pole of the Gaussian sphere, then the surface normal must lie on the northern hemisphere.[4] Each position of the viewer generates a fresh constraint hemisphere (see figure 4a). For known viewer movements these hemispheres can be intersected—the resultant patch on the Gaussian sphere places a tighter constraint on $\mathbf{n}$ (figure 4b). Clearly, motion that rotates by 180° about the object determines the surface normal, provided, of course, the point is always visible. The point will not be visible if another part of the surface occludes it, or if it has reached the extremal boundary (the back projection of the apparent contour in the image). However, when it reaches the extremal boundary the normal is fully determined [1].

The viewer motion must be accurately known in order to fully utilize the visibility constraint over a sequence of views. Uncertainty in motion could be included in a primitive fashion by intersecting regions larger than a hemisphere. The excess over a hemisphere can be bounded by estimates of error in viewer motion.

The constraint on the normal provided by the visibility constraint is applicable to texture points as well as smooth curves. The following constraint exploits the continuity of the curve.

4.2 Tangency constraint

The space curve tangent lies in the surface tangent plane and this constrains the surface normal $\mathbf{n}$:

$$\mathbf{T} \cdot \mathbf{n} = 0 \tag{18}$$

This orthogonality condition generates a constraint curve which is a great circle on the Gaussian sphere

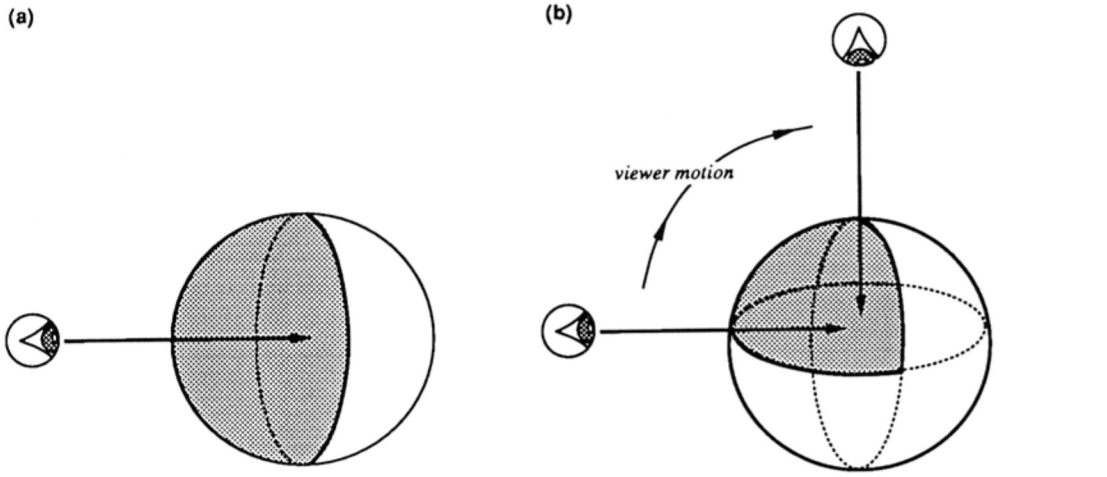

Fig. 4. The visibility constraint. (a) The visibility constraint restricts the surface normal $\mathbf{n}$ to lie on a hemisphere of the (Gauss map) Gaussian sphere. (b) By intersecting these constraint regions for known viewer motions a tighter constraint is placed on the normal.

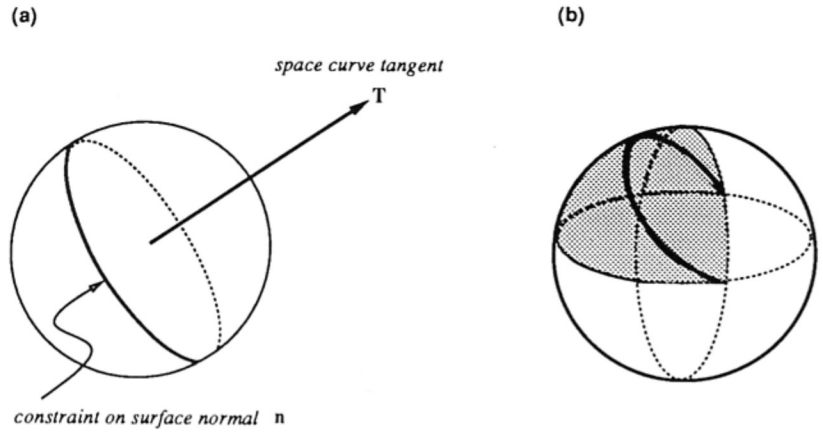

Fig. 5. The tangency constraint. (a) The tangent constraint restricts the surface normal to lie on a great circle of the Gaussian sphere. (b) By intersecting this curve with the constraint patch from the visibility constraint, the surface normal is further restricted to an arc of a great circle.

(figure 5a) [2]. If the curve tangent could be determined exactly, then intersecting the great circle with the constraint patch from the visibility constraint would restrict the normal to an arc of a great circle (figure 5b). In practice there will be errors in the tangent so the constraint region will be a band rather than a curve. Combining information from many views will more accurately determine the tangent (and hence the constraint band). However, no "new" information is generated in each view as it is using the visibility constraint.

4.3 Sign of Normal Curvature at Inflections

Even if the curvature and Frenet frame of a space curve lying on a surface are known, no constraint is placed on the surface curvature because the relation of the surface normal to the curve's osculating plane is unknown and arbitrary. However, it is shown below that at an inflection in the image curve, the sign of the *normal* curvature along the curve can be determined without first determining the surface normal.[5] Moreover it can be determined without having to recover the space curve. It is shown that by following the inflection through a sequence of images, the sign of the normal curvature is determined along the curve. This can be done with incomplete, qualitative knowledge of viewer motion. The only requirement is knowing whether the viewer is translating to the left or right of the image contour. This result is a generalization to surface curves of Weinshall's [28] result for surface texture.

Theorem 1 (Sign of normal curvatures from the deformation of inflections)
Consider two views of a curve lying on a smooth surface. If a point P on the curve projects to an inflection in one view, but not in the other, then the normal curvature (in the direction of the curve's tangent) at P is convex (concave) if the image of the curve at P has positive (negative) image curvature, κ^p, *in the second view.*[6] *The parameterization of the curve is chosen so that* $\mathbf{U}^p \cdot \mathbf{n}^p > 0$, *where* $\mathbf{U}^p$ *is the projection in the image of the translational velocity of the viewer. With the parameterization* sign $(\kappa^{\mathbf{n}}) = -$ sign $(\kappa_t^{\mathbf{p}})$ *where* κ^n *is the normal cuvature and* k_t^p *the time derivative of image curvature at the inflection.*

The proof below is in three stages. First, the viewing geometry is established (curve viewed in osculating plane, so it may be thought of as a plane curve). This determines $\mathbf{B} = \pm\mathbf{n}^p$ and hence constrains $\mathbf{N}$. Second, the sign of $\mathbf{N} \cdot \mathbf{Q}$ is determined from the time derivative of image curvature (this determines whether the curve bends toward or away from the viewing direction), see figure 6. Third, the visibility constraint is utilized to relate space curve curvature (the bending) to surface normal curvature, see figure 7.

Parameterization: The directions of the tangent vectors, $\mathbf{T}$, $\mathbf{t}^p$ and the image curve normal, $\mathbf{n}^p$, are arbitrarily defined by choosing the parameterization direction for the image curve. A convenient parameterization is to choose the direction of the curve normal so that it is on the same side of the image contour as the projection of the translational velocity, that is, $\mathbf{U}^p \cdot \mathbf{n}^p > 0$.

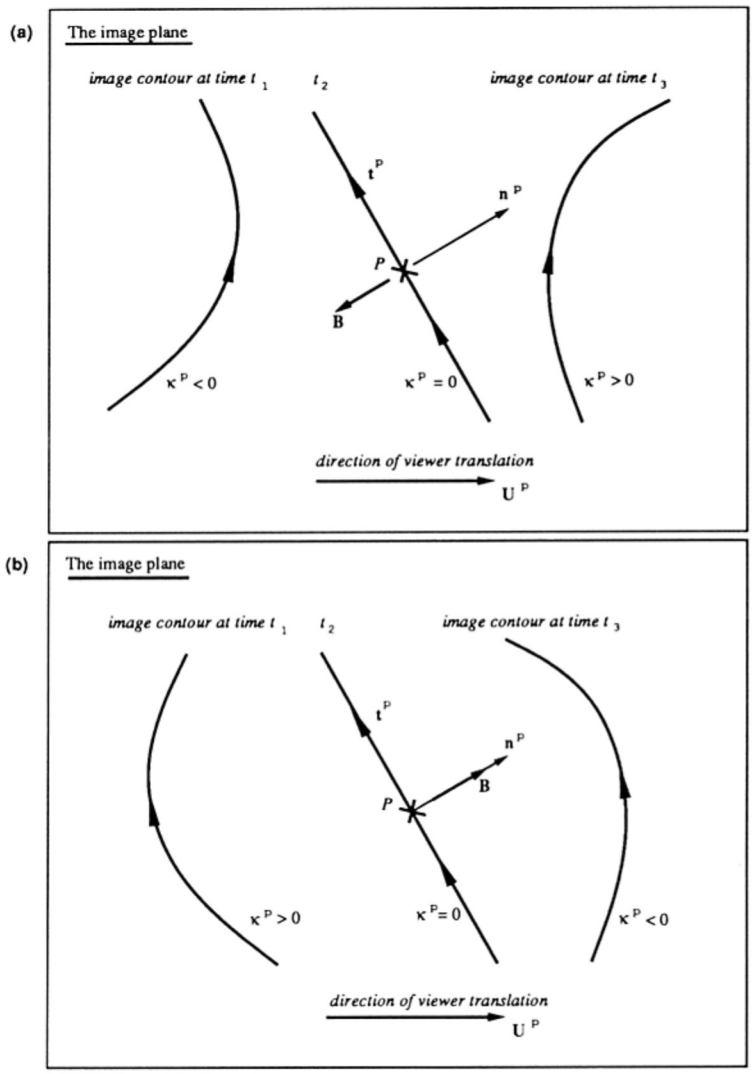

Fig. 6. Orientation of the space curve from the deformation at inflections. If the viewer crosses the osculating plane of the surface curve the curvature of the image will change sign—projecting to an inflection when the viewer lies in osculating plane (time t_2). Two possible cases are shown. (a) If $\mathbf{N} \cdot \mathbf{Q} > 0$ the space curve is bending away from the viewer (see figure 7a) and the image curve changes locally from an arc with negative image curvature via an inflection to an arc with positive image curvature, i.e., $\kappa_t^p > 0$. (b) If $\mathbf{N} \cdot \mathbf{Q} < 0$ the space curve is bending towards the viewer (see figure 7b) and the opposite transition is seen in the image, i.e., $\kappa_t^p < 0$.

This is always a good choice since it only fails when $\mathbf{U}^p \cdot \mathbf{n}^p = 0$ in which case the viewer is moving in the osculating plane and both views contain an inflection for the same point on the space curve. Since $\{\mathbf{Q}, \mathbf{t}^p, \mathbf{n}^p\}$ form an orthonormal right-handed system (with $\mathbf{Q}$ into the image plane), fixing the direction of the curve normal $\mathbf{n}^p$ also fixes $\mathbf{t}^p$ and hence $\mathbf{T}$ and the sign of κ^p.

Proof: We first establish a relation between $\mathbf{N} \cdot \mathbf{Q}$ and $\mathbf{B} \cdot \mathbf{n}^p$. From (11)

$$\mathbf{T} = \alpha \mathbf{t}^p + \beta \mathbf{Q} \quad \text{with } \alpha > 0 \tag{19}$$

Then

$$\begin{aligned} \mathbf{N} \cdot \mathbf{Q} &= \mathbf{Q} \cdot (\mathbf{B} \wedge \mathbf{T}) \\ &= \mathbf{B} \cdot (\mathbf{T} \wedge \mathbf{Q}) \\ &= \alpha \mathbf{B} \cdot (\mathbf{t}^p \wedge \mathbf{Q}) \\ &= -\alpha \mathbf{B} \cdot \mathbf{n}^p \end{aligned} \tag{20}$$

The last steps follow from (19) and (12), and since $\alpha > 0$,

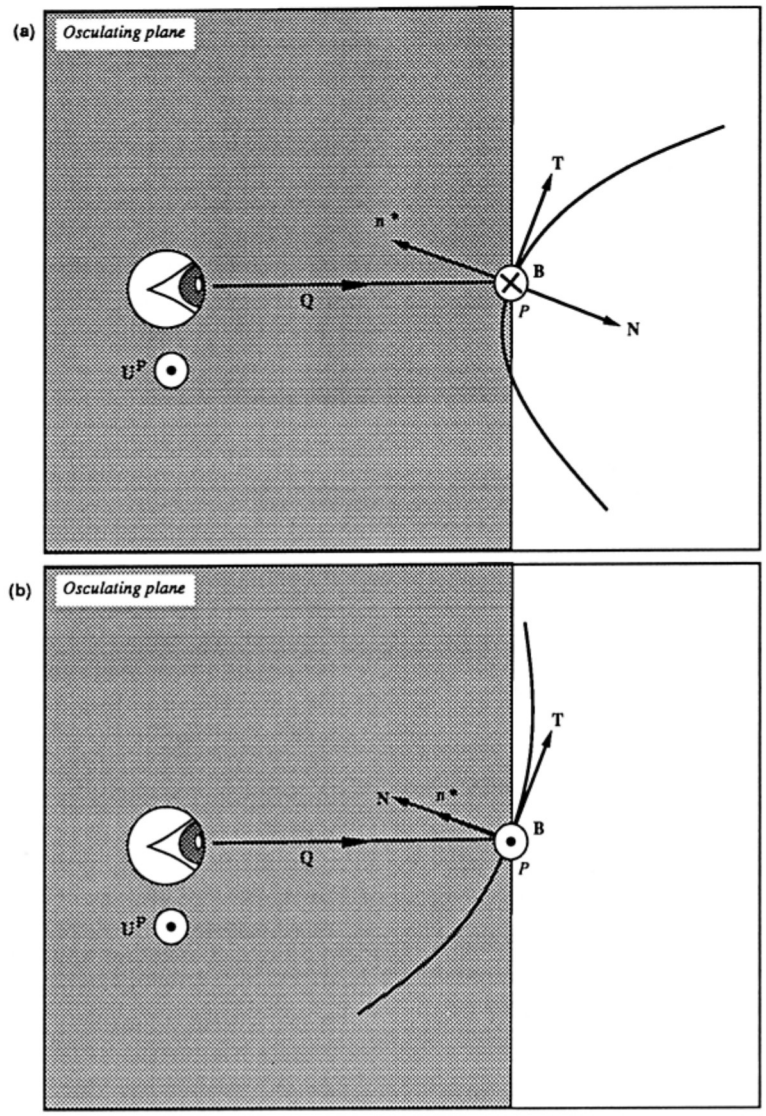

Fig. 7. Sign of normal curvature from osculating plane geometry. The component of the surface normal in the osculating plane ($\mathbf{n}^*$) is constrained to lie within 90° of the ray, $\mathbf{Q}$, by the visibility constraint ($\mathbf{n} \cdot \mathbf{Q} \leq 0$, shown shaded) and must be perpendicular to the surface curve tangent, $\mathbf{T}$ by the tangency constraint ($\mathbf{T} \cdot \mathbf{n} = 0$). The component of the surface normal in the osculating plane will therefore be parallel to the curve normal $\mathbf{N}$—either in opposite directions (a) if $\mathbf{N} \cdot \mathbf{Q} > 0$, or (b) in the same direction if $\mathbf{N} \cdot \mathbf{Q} < 0$. The sign of the normal curvature in the direction of the curve tangent is determined by the sign of $\mathbf{N} \cdot \mathbf{Q}$ which is obtained by noting the transition in image curvature at an inflection (see figure 6).

$$\text{sign}\,(\mathbf{N} \cdot \mathbf{Q}) = -\text{sign}\,(\mathbf{B} \cdot \mathbf{n}^p) \tag{21}$$

1. *Osculating plane constraints*
   If a point on a surface curve projects to an inflection in one view, but not in another then (from section 2.3.1) the ray in the first view must lie in the osculating plane, and from (14)

$$\mathbf{B} \cdot \mathbf{Q} = 0 \tag{22}$$

Since $\mathbf{B} \cdot \mathbf{T} = 0$ we have, from (19),

$$\mathbf{B} \cdot \mathbf{t}^p = 0 \tag{23}$$

Thus, using the orthogonal triad $\{\mathbf{Q}, \mathbf{t}^p, \mathbf{n}^p\}$

$$\mathbf{B} = \pm(\mathbf{Q} \wedge \mathbf{t}^p) \tag{24}$$

$$\mathbf{B} = \pm\mathbf{n}^p \tag{25}$$

2. *Sign of* $\mathbf{N} \cdot \mathbf{Q}$
The transition in image curvature at P from a point of inflection in the first view ($\kappa^p = 0$) to an arc with positive or negative image curvature, κ^p, in the second view determines the sign of $\mathbf{N} \cdot \mathbf{Q}$ (figure 6). We can express $\mathbf{U}$ in the orthogonal triad $\{\mathbf{Q}, \mathbf{t}^p, \mathbf{n}^p\}$ as

$$\mathbf{U} = \gamma \mathbf{n}^p + \delta \mathbf{t}^p + \epsilon \mathbf{Q} \quad \text{with } \gamma > 0 \tag{26}$$

the sign of γ follows from the parameterization choice that $\mathbf{U}^p \cdot \mathbf{n}^p > 0$. Using (22) an (23) gives

$$\mathbf{B} \cdot \mathbf{U} = \gamma \mathbf{B} \cdot \mathbf{n}^p \tag{27}$$

and hence from (16) (noting that κ and the denominator are positive),

$$\begin{aligned} \text{sign } (\kappa_t^p) &= -\text{sign } (\mathbf{B} \cdot \mathbf{U}) \\ &= -\text{sign } (\mathbf{B} \cdot \mathbf{n}^p) \\ &= \text{sign } (\mathbf{N} \cdot \mathbf{Q}) \end{aligned} \tag{28}$$

the last step following from (21). The result determines the orientation of the curve normal, $\mathbf{N}$, relative to the line of sign (figure 7).

3. *Sign of* κ^n
We express the surface normal $\mathbf{n}$ in the orthogonal triad $\{\mathbf{T}, \mathbf{N}, \mathbf{B}\}$:

$$\mathbf{n} = \hat{\alpha} \mathbf{N} + \hat{\beta} \mathbf{B} \tag{29}$$

since from (18) $\mathbf{T} \cdot \mathbf{n} = 0$. Hence, $\mathbf{Q} \cdot \mathbf{n} = \hat{\alpha} \mathbf{N} \cdot \mathbf{Q}$ since from (22) $\mathbf{B} \cdot \mathbf{Q} = 0$. The visibility constraint restricts the sign as $\mathbf{Q} \cdot \mathbf{n} \leq 0$, and hence sign $(\mathbf{N} \cdot \mathbf{Q}) = -\text{sign } (\hat{\alpha})$. The sign of the normal curvature κ^n then follows from the above and (28):

$$\begin{aligned} \text{sign } (\kappa^n) &= \text{sign } (\mathbf{N} \cdot \mathbf{n}) \\ &= \text{sign } (\hat{\alpha}) \\ &= -\text{sign } (\mathbf{N} \cdot \mathbf{Q}) \\ &= -\text{sign } (\kappa_t^p) \end{aligned} \tag{30}$$ □

Note that the test is only valid if the inflection in the first view moves along the image curve in the next view since an inflection corresponding to the same point on the surface curve in both views can result from either zero normal curvature or motion in the osculating plane. Two views of a surface curve are then sufficient to determine the sign of the normal curvature. However, because of the numerical difficulties in determining a zero of curvature, the test can be applied with greater confidence if a transition from (say) negative to zero (an inflection) to positive image curvature is observed. The component of viewer translation parallel to the image plane is only used to determine the direction of the curve parameterization. No knowledge of viewer rotations are required. The theorem is robust in that only partial knowledge (or inaccurate knowledge but with bounded errors) of translational velocity will suffice. This can be estimated from image measurements by motion parallax [21, 24] or is readily available in the case of binocular vision (where the camera or eye positions are constrained).

Applications

Figures 8–10 show examples of the application of this result to real images.

1. *Determining the sign of normal curvature by tracking inflections*
Figure 8 shows a sequence of images taken by a CCD camera mounted on an Adept robot arm rotating around a vase. Two image curves are selected—the projection of surface curves on the neck (hyperbolic patch) and body (elliptic path) of the vase respectively. These image curves are automatically tracked using B-spline snakes [11]. Crosses mark inflection points. As the viewer moves from left to right the inflections moves smoothly along each curve. For the curve on the hyperbolic section of the vase the transition in image curvature is from positive to negative indicating a concave normal section. For the curve on the elliptic section the transition is the reverse indicating a convex normal section. The main advantage is that provided the position of the inflection in one view can be identified with a convex or concave arc in the second—say by a nearby texture point—then only partial knowledge of the viewer motion is needed. In the case shown the only knowledge required is whether the viewer translation is to the left or right of the image contours.
2. *Convexity/concavity of test surface*
The test directly rules out certain types of surfaces as follows. If the normal curvature is negative then the surface could be convex or hyperbolic—it cannot be concave. Similarly, a positive normal curvature rules out a convex surface. Thus the result can be used as a test for nonconvexity or nonconcavity. This is similar to the information available from the motion of a specularity when the light source position is not known [30].

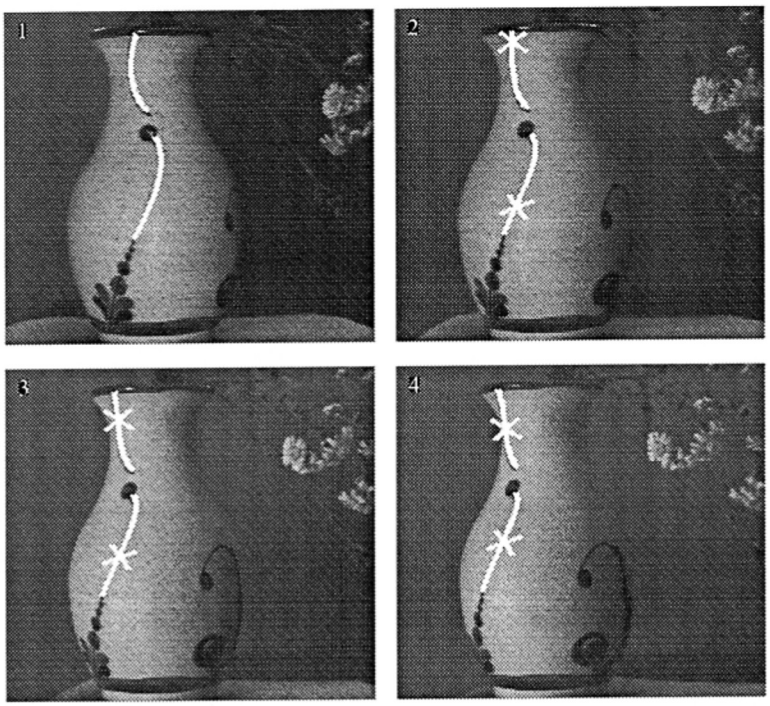

Fig. 8. Tracking inflections to determine the sign of normal curvature. Four images are shown from an image sequence taken by a camera moving (from left to right with fixation) around a smooth surface (a vase). The image contours are tracked by using B-spline snakes. Inflections (marked by a cross) are generated for points whose osculating plane contains the vantage point. Under viewer motion the preimage of the inflection moves along the surface curve. The change in the sign of image curvature is sufficient to determine the sign of the normal curvature along the curve. For the top part of the curve on the neck of the vase the transition in image curvature is from positive to negative indicating concave normal sections along the curve. For the bottom part of the curve on the body of the vase the transition is the opposite, indicating convex normal sections. This information is consistent with the neck of the vase being hyperbolic and the body convex elliptic. Note that this classification has been achieved with partial knowledge of the viewer motion. The only knowledge required is whether the component of viewer translation parallel to the image plane is to the left or right of the image contours.

3. *Combination with other cues*
   The test is most powerful when combined with other cues. Extremal boundaries, for example, are an extremely rich source of surface shape information. Unfortunately they cannot provide information on concave surface patches since these will never appear as extremal boundaries. The information available from the deformation of surface curves is therefore extremely important even though it is not as powerful a cue as the image of the extremal boundary. For example at an extremal boundary the Gaussian curvature of the surface is known from the sign of the curvature of the apparent contour in the image. Consider an elliptic region (this must be convex to appear on the extremal contour, if there is a point P inside the extremal boundary with concave (positive) normal curvature (determined using the test above), then there must be at least one parabolic curve between P and the boundary.

   This information can be used, for example, to indicate the presence of concavities for grasping. Figure 9 shows an example of a Japanese tea cup. The application of the test to the image contour of the Chinese character (tracked by a B-spline snake) in the indentation indicates the presence of concavity. These concavities (thumb imprints) are deliberately placed by Japanese potters when making tea cups since they aid in grasping the cup.
4. *Interpreting single images of planar curves*
   It is well known that by making certain assumptions about the nature of the surface curves humans can interpret the shape of visible surfaces from single images of surface curves. Typically this has been used to infer the orientation of planar surfaces. Stevens [25] has shown how the assumptions of parallel contour generators (with the implicit assumption that the curvature perpendicular to the contour is a principal curvature with zero curvature)

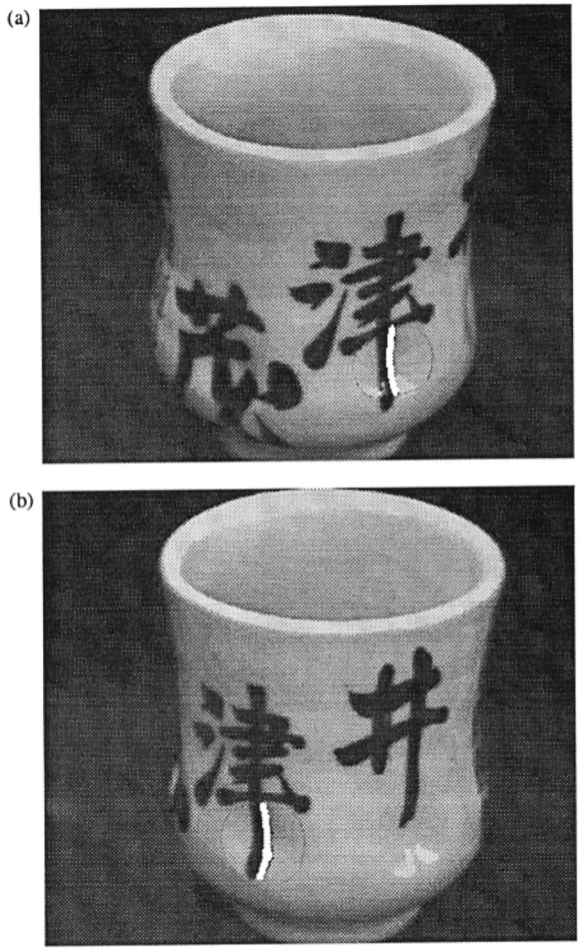

Fig. 9. Qualitative information for grasping. The left and right images of a Japanese tea cup are shown. The simple test can be used for the Chinese characters painted in the indentations created by the potter's thumb imprints. The transition in the sign of image curvature from positive to negative (the transitional view containing the inflections is not shown) indicates a concave section. These thumb imprints are created to aid in grasping the tea cup.

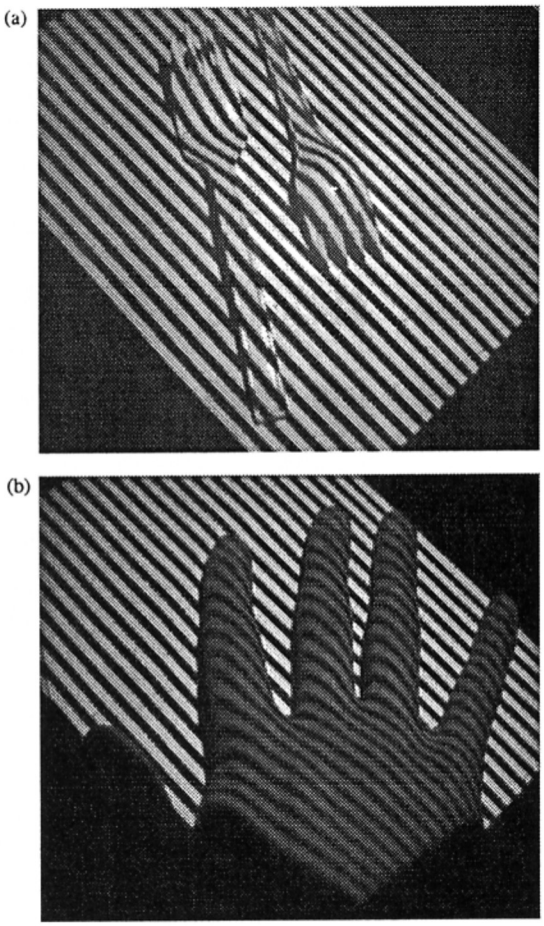

Fig. 10. Qualitative interpretation of rangefinder images. These images were formed by the projection of planes of light onto the workspace and viewing the scene with a camera whose center is displaced to the *left* of the light plane. The surface is covered artificially with a set of planar curves. If these surface curves were viewed in their respective osculating plane (the light planes) their images would simply be straight lines (degenerate case of an inflection). The sign of the image curvature in the images shown is consistent with the sign of the normal curvatures along the curve. Positive, negative and zero image curvature indicate respectively convex, concave and planar surface sections.

can be used to recover the shape of curved surfaces. The result described above can be used to make precise the intuition of Stevens that the appearance of planar surface curves directly constrains the shape of the surface. This is highlighted with a simple example based on the qualitative interpretation of range-finder images. Figure 10 shows two images taken with a rangefinder system [4]. The images are formed by the projection of planes of light on to the workspace and viewing this scene with another camera whose center is displaced away from the light plane. The effect is to cover the untextured surface with planar surface curves. The osculating plane of these curves is simply the light plane. If the camera is placed in the osculating plane the light stripes would appear as straight lines in the image. (The straight line is simply a degenerate case of an inflection.) By taking an image with the camera on one side of the osculating plane (the light plane) the straight lines deform in a way predicting by the test above. The sign of the image curvature is consistently related to the sign of the normal curvature

along the curve. In the examples of figure 10 the camera is displaced to the left of the light-plane projector and positive, negative, and zero image curvature (straight lines) indicate respectively convex, concave, and zero normal curvatures. The cue is extremely powerful, giving a strong sense of the shape of the visible surfaces without the need for accurate image measurements, exact epipolar geometry, and triangulation which are required in the established, quantitative approach for interpreting rangefinder images.

Similar effects can be observed in the shadows cast by sunlight through venetian blinds.

4.4 Surface Curvature at Curve Intersections

If surface curves cross transversely, or the curve's tangent is discontinuous, more constraints can be placed on the surface geometry. In principle from two views it is possible to reconstruct both space curves and hence determine their tangents and curvatures at the intersection. From these the normal curvatures $\kappa^{n(1)}$, $\kappa^{n(2)}$ along the two tangent directions can be determined

$$\kappa^{n(1)} = \kappa^{(1)}\mathbf{N}^{(1)} \cdot \mathbf{n} \tag{31}$$

$$\kappa^{n(2)} = \kappa^{(2)}\mathbf{N}^{(2)} \cdot \mathbf{n} \tag{32}$$

where $\mathbf{n}$ is the surface normal

$$\mathbf{n} = \frac{\mathbf{T}^{(1)} \wedge \mathbf{T}^{(2)}}{\|\mathbf{T}^{(1)} \wedge \mathbf{T}^{(2)}\|} \tag{33}$$

and $\kappa^{(i)}$, $\mathbf{T}^{(i)}$ $i = 1, 2$ are the curvature, tangent, and normals of the space curves at the intersection. An intersection of the two curves ensures sufficient information to recover the surface normal. It has the added advantage that the exact epipolar geometry is not required to match points in the two images since the intersection can be tracked. It also has the advantage that the surface normal can be computed by measuring the change in curve normals; we need only know the orientation of the viewer in order to compute $\mathbf{Q}(s, t)$—translation is not required. This is done by applying (59) to recover both space curve tangents and taking their vector product to determine the surface normal (33).

However, the recovery of two normal curvatures is not sufficient in general to determine the Gaussian curvature of the surface (there are many convex and concave directions on a hyperbolic patch). It can only constrain its sign. The problem is that although the angle between the tangent vectors is known, the relation between the tangent pair and the principle directions is unknown. From Euler's formula [12] we have

$$\kappa^{n(1)} = \kappa_1 \sin^2 \theta + \kappa_2 \cos^2 \theta \tag{34}$$

$$\kappa^{n(2)} = \kappa_1 \sin^2 (\theta + \alpha) + \kappa_2 \cos^2 (\theta + \alpha) \tag{35}$$

where α is the known angle between the tangents in the tangent plane; θ is the (unknown) angle between the tangent, $\mathbf{T}^{(1)}$, and the *principal* direction; κ_1 and κ_2 are the principal curvatures. There are three unknowns, κ_1, κ_2, θ, and only two constraints. If there is a triple crossing or higher there are sufficient constraints to uniquely determine the three unknowns. This is less likely to occur. However, we can catalogue the surface by the sign of the Gaussian curvature.

Sign of $\kappa^{n(1)}$ and $\kappa^{n(2)}$	Surface
both negative	*not* concave
both positive	*not* convex
one negative, one positive	hyperbolic

Furthermore, it is straighforward to show that there is a lower bound on the difference of the principle curvatures, namely

$$|\kappa_1 - \kappa_2| \geq \left| \frac{\kappa^{n(1)} - \kappa^{n(2)}}{\sin \alpha} \right| \tag{36}$$

where α is the angle between the tangents in the tangent plane and $\kappa^{n(i)}$ are measured normal curvatures.

Proof: Subtracting the two copies of (34) for the curvatures of the two curves and simple trigonometry gives

$$\kappa^{n(1)} - \kappa^{n(2)} = (\kappa_1 - \kappa_2)(\sin \alpha \sin (\alpha + 2\theta)) \tag{37}$$

Rearranging and inspecting the magnitude of both sides gives the required result.

This is simply repackaging the information contained in the normal curvatures and the angle between tangents. However, in this form it is better suited to a first filter on a model data base. For example if it were known that the model was convex a negative sign test would reject it. Similarly if the principle curvatures were known not to exceed certain limits, then the lower bound test might exclude it.

5 Discussion

Surprisingly—even with exact epipolar geometry and accurate image measurements—very little quantitative

information about local surface shape is directly recoverable from surface curves. This is in sharp contrast to the extremal boundaries of curved surfaces in which a single image can provide strong constraints on surface shape while a sequence of views allows the complete specification of the surface. However the apparent contours cannot directly indicate the presence of concavities. The image of surface curves is therefore an important cue.

The information available from image curves is better expressed in terms of incomplete, qualitative constraints on surface shape. It has been shown that visibility of the curve constrains surface orientation and moreover that this constraint improves with viewer motion. Furthermore, tracking image curve inflections determines the sign of normal curvature along the surface curve's tangent. This can also be used to interpret the images of planar curves on surfaces—making precise Stevens' intuition that we can recover surface shape from the deformed image of a planar curve. This information is robust in that it does not require accurate measurements or the exact details of viewer motion.

Additional constraints may be derived by metric information, as well as by the sign of curvature, and by extending the visibility constraint to incorporate multilocal events.

Acknowledgments

We are grateful to Andrew Blake, Mike Brady, and Peter Giblin for helpful comments. The support of the IBM UK Scientific Centre, St. Hugh's College and the Toshiba Corporation (for RC), the SERC (for AZ), and the University of Oxford are gratefully acknowleged.

References

1. H.G. Barrow and J.M. Tenenbaum, Interpreting line drawings as three-dimensional surfaces, *Artificial Intelligence*, 17:75–116, 1981.
2. A. Blake, Ambiguity of shading and stereo contour, *Proc. Alvey Vis. Conf.* pp. 97–105, 1987.
3. A. Blake and R. Cipolla, Robust estimation of surface curvature from deformation of apparent contours, *Proc. 1st Europ. Conf. Comput. Vis.* pp. 465–474. France (Springer-Verlag), 1990.
4. A. Blake, D.H. McCowen, H.R. Lo, and D. Konash, Trinocular active range-sensing. *Proc. 1st British Mach. Vis. Conf.*, pp. 19–24, 1990.
5. R.C. Bolles, H.H. Baker, and D.H. Marimont, Epipolar-plane image analysis: An approach to determining structure, *Intern. J. Comput. Vis.* 1:7–55, 1987.
6. M. Brady, J. Ponce, A. Yuille, and H. Asada. Describing surfaces, *Comput. Vis. Graph. Image Process.* 32:1–28, 1985.
7. J.W. Bruce and P.J. Giblin. *Curves and Singularities.* Cambridge University Press: Cambridge, 1984.
8. J.W. Bruce and P.J. Giblin. Outlines and their duals, *Proc. London Math Soc.*, pp. 552–570, 1985.
9. J.F. Canny, A computational approach to edge detection, *IEEE Trans. Patt. Anal. Mach. Intell.* 8:679–698, 1986.
10. R. Cipolla, Active Visual Inference of Surface Shape, Ph.D. thesis, University of Oxford, 1991.
11. R. Cipolla and A. Blake, The dynamic analysis of apparent contours, *Proc. 3rd Intern. Conf. Comput. Vis.* Osaka, pp. 616–623, 1990.
12. M.P. DoCarmo. *Differential Geometry of Curves and Surfaces.* Prentice-Hall: Englewood Cliffs, NJ, 1976.
13. O.D. Faugeras, On the motion of 3D curves and its relationship to optical flow, *Proc. 1st Europ. Conf. Comput. Vision*, France, 1990.
14. P.J. Giblin and R. Weiss, Reconstruction of surfaces from profiles, *Proc. 1st Intern. Conf. Comput. Vis.*, London, pp. 136–144, 1987.
15. W.E.L. Grimson. *From Images to Surfaces.* MIT Press: Cambridge, MA, 1981.
16. B.K.P. Horn, *Robot Vision.* McGraw-Hill: New York, 1986.
17. B.K.P. Horn, Closed-form solution of absolute orientation using unit quanternions, *J. Opt. Soc. Amer.* A4(4):629–624, 1987.
18. M. Kass, A. Witkin, and D. Terzopoulos. Snakes: active contour models. *Proc. 1st Intern. Conf. Comput. Vis.* London, pp. 259–268, 1987.
19. J.J. Koenderink, What does the occluding contour tell us about solid shape? *Perception* 13:321–330, 1984.
20. J.J. Koenderink. *Solid Shape.* MIT Press: Cambridge, MA, 1990.
21. H.C. Longuet-Higgins and K. Pradzny, The intepretation of a moving retinal image, *Proc. Roy. Soc. London* B208:385–397, 1980.
22. S.J. Maybank, The angular velocity associated with the optical flow field arising from motion through a rigid environment, *Proc. Roy. Soc. London* A401:317–326, 1985.
23. N. Navab, N. Deriche, and O.D. Faugeras, Recovering 3D motion and structure from stereo and 2D token tracking cooperation, *Proc. 3rd Intern. Conf. Comput. Vis.*, Osaka, pp. 513–516, 1990.
24. J.H. Rieger and D.L. Lawton, Processing differential image motion, *J. Opt. Soc. Amer.* A2(2), 1985.
25. K.A. Stevens, The visual intepretation of surface contours, *Artificial Intelligence* 17:47–73, 1981.
26. R. Vaillant, Using occluding contours for 3D object modelling, *Proc. 1st Europ. Conf. Comput. Vis.*, France, pp. 454–464, 1990.
27. A. Verri and A. Yuille, Some perspective projection invariants, *J. Opt. Soc. Amer.* A5(3):426–431, 1988.
28. D. Weinshall, Direct computation of 3D shape and motion invariants, *Proc. 3rd Intern. Conf. Comput. Vis.*, Osaka, pp. 230–237, 1990.
29. D. Weinshall, Qualitative depth from stereo, with applications, *Comput. Vis. Graph. Image Proccess.* 49:222–241, 1990.
30. A. Zisserman, P.J. Giblin, and A. Blake. The information available to a moving observer from specularities. *Image Vis. Comput.* 7(1):38–42, 1989.

Appendix A: Projection of Space Curves

Relationship Between Image Curve and Space Curve Tangents

The image of a world point, P, with position vector, $\mathbf{r}(s)$, is a unit vector $\mathbf{Q}(s, t)$ such that

$$\mathbf{r}(s) = \mathbf{v}(t) + \lambda(s, t)\mathbf{Q}(s, t)$$

Differentiating with respect to the curve parameter, s,

$$\mathbf{r}_s = \lambda_s \mathbf{Q} + \lambda \mathbf{Q}_s \tag{38}$$

and rearranging we derive the following relationships:

$$\mathbf{Q}_s = \frac{\mathbf{Q} \wedge (\mathbf{r}_s \wedge \mathbf{Q})}{\lambda} \tag{39}$$

$$|\mathbf{Q}_s| = \frac{|\mathbf{r}_s|}{\lambda} \left(1 - \left(\mathbf{Q} \cdot \frac{\mathbf{r}_s}{|\mathbf{r}_s|} \right)^2 \right)^{1/2} \tag{40}$$

Note that the mapping from space curve to the image contour is singular (degenerate) when the ray and curve tangent are aligned. The tangent to the space curve projects to a point in the image and a *cusp* is generated in the image contour.

By expressing (39) in terms of unit tangent vectors, $\mathbf{t}^p$ (tangent to the spherical image curve) and $\mathbf{T}$ (space curve tangent) we have

$$\begin{aligned} \mathbf{t}^p &= \frac{\mathbf{Q}_s}{|\mathbf{Q}_s|} \\ &= \frac{\mathbf{Q} \wedge (\mathbf{T} \wedge \mathbf{Q})}{(1 - (\mathbf{Q} \cdot \mathbf{T})^2)^{1/2}} \\ &= \frac{\mathbf{T} - (\mathbf{Q} \cdot \mathbf{T})\mathbf{Q}}{(1 - (\mathbf{Q} \cdot \mathbf{T})^2)^{1/2}} \end{aligned}$$

Relationship Between Image and Space Curve Curvature

Differentiating (38) with respect to s and collecting the components parallel to the image curve normal, $\mathbf{n}^p$, gives

$$\mathbf{Q}_{ss} \cdot \mathbf{n}^p = \frac{\mathbf{r}_{ss} \cdot \mathbf{n}^p}{\lambda} \tag{41}$$

Substituting this and (40) into the expression for the curvature of the image curve (13) gives

$$\begin{aligned} \kappa^p &= \frac{\mathbf{r}_{ss} \cdot \mathbf{n}^p}{\lambda |\mathbf{Q}_s|^2} \\ &= \lambda\kappa \frac{\mathbf{N} \cdot \mathbf{n}^p}{(1 - (\mathbf{Q} \cdot \mathbf{T})^2)} \end{aligned} \tag{42}$$

Substituting (12) and (11) for $\mathbf{n}^p$ gives the desired relationship:

$$\kappa^p = \lambda\kappa \frac{\mathbf{N} \cdot (\mathbf{Q} \wedge \mathbf{t})}{(1 - (\mathbf{Q} \cdot \mathbf{T})^2)^{3/2}} \tag{43}$$

$$= \lambda\kappa \frac{\mathbf{B} \cdot \mathbf{Q}}{(1 - (\mathbf{Q} \cdot \mathbf{T})^2)^{3/2}} \tag{44}$$

Appendix B: Deformation of Image Curve Due to Viewer Motion

Viewer and Reference Coordinate Systems

For a moving observer the viewer (camera) coordinate is continuously changing with respect to the fixed coordinate system used to describe R^3. Note that $\mathbf{Q}$ is the direction of the light ray in the fixed reference/world frame for R^3. It is determined by a spherical image position vector $\tilde{\mathbf{Q}}$ (the direction of the ray in the camera/viewer coordinate system) and the orientation of the camera coordinate system relative to the reference frame. The relationship between the measurements in the two frames, $\mathbf{Q}$ and $\tilde{\mathbf{Q}}$, can be conveniently expressed in terms of a rotation operator $R(t)$ [17]:

$$\mathbf{Q} = R(t)\tilde{\mathbf{Q}} \tag{45}$$

The frames are defined so that instantaneously, at time $t = 0$, they coincide:

$$\mathbf{Q}(s, 0) = \tilde{\mathbf{Q}}(s, 0) \tag{46}$$

and have relative translational and rotational velocities of $\mathbf{U}(t)$ and $\Omega(t)$ respectively:

$$\mathbf{U} = \mathbf{v}_t \tag{47}$$

$$(\Omega \wedge \tilde{\mathbf{Q}}) = R_t \tilde{\mathbf{Q}} \tag{48}$$

where subscripts denote differentiation with respect to time. The relationship between temporal derivatives of measurements made in the camera coordinate system and those made in the reference frame is obtained by differentiating (45) and substituting (46). In particular the temporal derivative of the ray, the image curve

tangent, and the image curve normal, $\{\mathbf{Q}, \mathbf{t}^p, \mathbf{n}^p\}$, are related to temporal derivatives of the image curve measured in the viewer coordinate system, $\{\tilde{\mathbf{Q}}, \tilde{\mathbf{t}}^p, \tilde{\mathbf{n}}^p\}$, by

$$\mathbf{Q}_t = \tilde{\mathbf{Q}}_t + \Omega(t) \wedge \tilde{\mathbf{Q}} \tag{49}$$

$$\mathbf{t}_t^p = \tilde{\mathbf{t}}_t^p + \Omega(t) \wedge \tilde{\mathbf{t}}^p \tag{50}$$

$$\mathbf{n}_t^p = \tilde{\mathbf{n}}_t^p + \Omega(t) \wedge \tilde{\mathbf{n}}^p \tag{51}$$

Quantifying the Deformation

For a static space curve (not an extremal boundary of a curved surface) the position of a point P on the curve, $\mathbf{r}(s)$, does not change with time:

$$\mathbf{r}_t = 0 \tag{52}$$

This can be used to derive the relationship between the images of the point P in the sequence of views. Differentiating (10) with respect to t and substituting the condition (52) gives an infinitesimal analog of the epipolar constraint in which the ray is constrained to lie in the epipolar plane defined by the ray in the first view $\mathbf{Q}$ and the viewer translation $\mathbf{U}$ (figure 3):

$$\mathbf{Q}_t = \frac{(\mathbf{U} \wedge \mathbf{Q}) \wedge \mathbf{Q}}{\lambda} \tag{53}$$

In terms of measurements on the image sphere,

$$\tilde{\mathbf{Q}}_t = \frac{(\mathbf{U} \wedge \tilde{\mathbf{Q}}) \wedge \tilde{\mathbf{Q}}}{\lambda} - \Omega \wedge \tilde{\mathbf{Q}} \tag{54}$$

where $\tilde{\mathbf{Q}}_t$ is the image velocity of a point on the space curve at a distance λ. Equation (54) is the well known equation of structure from motion [22]. Points on successive image curves are "matched" by searching along epipolar great circles on the image sphere (or epipolar lines for planar image geometry) defined by the viewer motion, $\mathbf{U}$, Ω and the image position $\tilde{\mathbf{Q}}$. Note also that the image velocity consists of two components. One component is determined purely by the viewer's rotational velocity about camera center and is independent of the structure of the scene (λ). The other component is determined by the translational velocity of the viewer.

Depth from Image Velocities

Depth λ (distance along the ray $\mathbf{Q}$) can be computed from the deformation ($\mathbf{Q}_t$) of the image contour under known viewer motion [5, 16]. From (53),

$$\lambda = -\frac{\mathbf{U} \cdot \mathbf{n}^p}{\mathbf{Q}_t \cdot \mathbf{n}^p}. \tag{55}$$

This formula is an infinitesimal analog of triangulation with stereo cameras. The numerator is analogous to baseline and the denominator to disparity.

Equation (55) can also be re-expressed in terms of spherical image position $\tilde{\mathbf{Q}}$ and the normal component of image velocity $\tilde{\mathbf{Q}}_t \cdot \mathbf{n}^p$:

$$\lambda = -\frac{\mathbf{U} \cdot \mathbf{n}^p}{\tilde{\mathbf{Q}}_t \cdot \mathbf{n}^p + (\Omega \wedge \tilde{\mathbf{Q}}) \cdot \mathbf{n}^p} \tag{56}$$

Curve Tangent from Rate of Change of Orientation of Image Tangent

Having recovered the depth of each point on the space curve it is possible to recover the geometry of the space curve by numerical differentiation. Here, an alternative method is presented. This recovers the curve tangent and normal directly from image measurables without first explicitly recovering the space curve. The space curve tangent, $\mathbf{T}$, can be recovered from the temporal derivative of the image curve normal, $\mathbf{n}^p$, as follows.

It is straightforward to shown from (11) that

$$\mathbf{T} \cdot \mathbf{n}^p = 0 \tag{57}$$

Differentiating (57) with respect to time t gives

$$\mathbf{T} \cdot \mathbf{n}_t^p = 0 \tag{58}$$

since the space curve is assumed static and does not change with time. Equations (57) and (58) allow the recovery of the space curve tangent up to an arbitrary sign. In terms of measurements on the image sphere,

$$\mathbf{T} = \frac{\tilde{\mathbf{n}}^p \wedge (\tilde{\mathbf{n}}_t^p + \Omega \wedge \tilde{\mathbf{n}}^p)}{|\tilde{\mathbf{n}}^p \wedge (\tilde{\mathbf{n}}_t^p + \Omega \wedge \tilde{\mathbf{n}}^p)|} \tag{59}$$

The orientation of the space curve tangent is recovered from the change in the image curve normal and knowledge of the viewer's rotational velocity. An expression similar to (59) was derived by Navab, Deriche, and Faugeras [23] for the image motion of straight lines.

Curvature and Curve Normal

We now show how to recover the space curve's curvature, κ and normal, $\mathbf{N}$, directly from measurements on the spatiotemporal image and known viewer motion.

To simplify the derivation we choose a frame aligned with the curve normal with basis vectors $\{\mathbf{n}^p, \mathbf{n}_t^p, \mathbf{T}\}$. (It is easy to see from (57) and (58) that these three vectors are orthogonal. $\mathbf{n}_t^p$ is not necessarily a unit vector.) In this frame $\kappa\mathbf{N}$ can be expressed as

$$\kappa\mathbf{N} = \alpha\mathbf{n}^p + \beta\mathbf{n}_t^p + \gamma\mathbf{T} \tag{60}$$

From the definition of a space curve normal, γ must be zero. The other two orthogonal components of $\kappa\mathbf{N}$; $\kappa\mathbf{N} \cdot \mathbf{n}^p$ and $\kappa\mathbf{N} \cdot \mathbf{n}_t^p$, can be recovered from the curvature in the image (42) and its temporal derivative as follows. By rearranging (42) we can solve for α. Differentiating (42) and rearranging we can recover the other component, β [10]. The space curve normal and curvature can be recovered directly from measurements in the image and known viewer motion.

Temporal Derivative of Image Curvature

We now relate the space curve's curvature, κ, to the temporal derivative of the image curve's curvature, κ_t^p. Differentiating (14), substituting (53) and (14), and noting that for a fixed space curve (from (52))

$$\lambda_t + \mathbf{U} \cdot \mathbf{Q} = 0$$

we can derive

$$\kappa_t^p = -\frac{\kappa\mathbf{B} \cdot \mathbf{U}}{(1 - (\mathbf{Q} \cdot \mathbf{T})^2)^{3/2}} + \frac{3\kappa^p[(\mathbf{Q} \cdot \mathbf{T})(\mathbf{Q}_t \cdot \mathbf{T})]}{\lambda(1 - (\mathbf{Q} \cdot \mathbf{T})^2)^{1/2}}$$

Substituting (53) and (11) for $\mathbf{Q}t$ and $\mathbf{T}$ respectively:

$$\kappa_t^p = -\frac{\kappa\mathbf{B} \cdot \mathbf{U}}{(1 - (\mathbf{Q} \cdot \mathbf{T})^2)^{3/2}} - \frac{3\kappa^p[(\mathbf{Q} \cdot \mathbf{T})(\mathbf{U} \cdot \mathbf{t}^p)]}{\lambda(1 - (\mathbf{Q} \cdot \mathbf{T})^2)^{1/2}}$$

The temporal change in the image curvature for a point on a space curve depends on the viewer's motion relative to the curve's osculating plane.

Notes

1. The space curve $\mathbf{r}(s)$ is fixed on the surface and is view independent. This is the only difference between this and the spatio-temporal analysis of the family of contour generators (extremal boundaries) of a smooth curved surface $\mathbf{r}(s, t)$ [3, 11].
2. The *geodesic* curvature is the magnitude of the component of $\kappa\mathbf{N}$ perpendicular to the surface normal [12]. For a curve on the imaging sphere this direction is parallel to the curve normal, $\mathbf{n}^p$, and the *geodesic* curvature is equal to the curvature of the perspective projection onto a plane defined by the ray direction. It has a well-defined sign whereas it is meaningless to refer to the sign of curvature of a space curve.
3. An informal way to see this is to consider orthographic projection with the view direction defining a point $\mathbf{Q}$ on the Gaussian sphere. The tangent at each point on the space curve also defines a point on the Gaussian sphere, and so $\mathbf{T}_G(s)$ traces a curve. For a cusp, $\mathbf{Q}$ must lie on $\mathbf{T}_G(s)$ and this will not occur in general. However, a one parameter family of (orthographic) views $\mathbf{Q}(t)$ also defines a curve on the Gaussian sphere. Provided these cross (transversely) the intersection will be stable to perturbations in $\mathbf{r}(s)$ and viewpoint. For an inflection $\mathbf{Q}$ must lie in the osculating plane. This defines a great circle on the Gaussian sphere for each point of the space curve, and so covers a region for the curve $\mathbf{r}(s)$. If the point $\mathbf{Q}$ lies in this region the projection contains an inflection, and this will be stable to perturbations of $\mathbf{r}(s)$.
4. The convention used is that the surface normal is defined as being outward from the solid surface.
5. The *normal* curvature is the curvature of the planar section of the surface through the normal and tangent vector.
6. If we define the surface normal as being outward from the solid surface, the *normal* curvature will be negative in any direction for a convex surface patch.